

## Graphene as a Substrate To Suppress Fluorescence in Resonance Raman Spectroscopy

Liming Xie, Xi Ling, Yuan Fang, Jin Zhang,\* and Zhongfan Liu\*

Beijing National Laboratory for Molecular Sciences, Key Laboratory for the Physics and Chemistry of Nanodevices, State Key Laboratory for Structural Chemistry of Unstable and Stable Species, College of Chemistry and Molecular Engineering, Peking University, Beijing 100871, P. R. China

Received May 8, 2009; E-mail: jinzhang@pku.edu.cn

Resonance Raman spectroscopy (RRS), which can enhance Raman signal by  $10^7$  times than normal Raman spectroscopy, is a powerful approach to characterize structures of chemicals (especially biomolecules) at low concentrations.<sup>1–4</sup> However, fluorescence (FL) background is a major obstacle in RRS because the FL cross section ( $\sim 10^{-16}$  cm<sup>2</sup>) is much larger than the RRS cross section ( $\sim 10^{-22}$  cm<sup>2</sup>).<sup>3</sup> Several approaches, such as ultraviolet RRS (UV-RRS),<sup>1</sup> time-resolved Raman detection,<sup>5,6</sup> femtosecond broadband stimulated Raman spectroscopy (FSRS),<sup>7</sup> and coherent anti-Stokes Raman spectroscopy (CARS),<sup>8</sup> have been used to suppress or reject FL background in RRS. However, these approaches need expensive and complex equipments and have other limitations, such as sample degradation in UV-RRS. Surface-enhanced Raman spectroscopy (SERS) is another powerful approach to characterize structures of chemicals at extremely low concentrations or even at the single molecule level.<sup>9</sup> But the metal surfaces used in SERS require proper roughing and further modification for bioapplications.

Graphene, a plane of honeycomb carbon lattice, has attracted intense interests for its unusual properties<sup>10,11</sup> as a consequence of its linear energy dispersion near the Dirac points. Sp<sup>2</sup> carbon materials, like carbon nanotubes (CNTs), have excellent biocompatibility and have applications in biosensing<sup>12</sup> and drug delivery.<sup>13</sup> Graphene has a similar biocompatible surface and has potential bioapplications<sup>14,15</sup> too. Herein, we demonstrate that graphene can be used as a substrate to suppress FL background by  $\sim 10^3$  times (Figure 1a), which can be used to measure RRS from fluorescent molecules at low concentrations. Two probe molecules were used in this work: rhodamine 6G (R6G) and protoporphyrin IX (PPP) (chemical structures in Supporting Information (SI)).

Graphene was prepared by mechanical exfoliation of Kish graphite (Covalent Materials Corp.) on SiO<sub>2</sub>/Si (300 nm thick oxide). Raman measurement and optical imaging were used to identify monolayer (1L), bilayer (2L), and multilayer (ML) graphenes and graphite pieces<sup>16,17</sup> (see SI). Graphene on SiO<sub>2</sub>/Si was soaked in R6G solution (10 μM in water) or PPP solution (20 μM in methanol) for 30 min. Then the graphene sample with adsorbates was rinsed in the corresponding solvent for  $\sim 15$  min and then dried under a N<sub>2</sub> flow. A Horiba HR800 Raman system with a 514 and a 633 nm laser was used. A 100× objective was used to focus the laser beam and collect the Raman-FL signal. The laser power on the sample was  $\sim 0.6$  mW for 514 nm and 4 mW for 633 nm.

A typical Raman-FL spectrum of R6G in solution at 514 nm excitation is shown in Figure 1b (the blue line). Only a strong FL background was observed. The Raman peaks, whose intensity should be above the detection limit of our system,<sup>3</sup> however, were not observed due to the strong shot noise of the FL emission. The wave pattern with a period of  $\sim 100$  cm<sup>-1</sup> shown in the Raman-FL spectra (blue line in Figure 1b and line in Figure 2a) is due to the

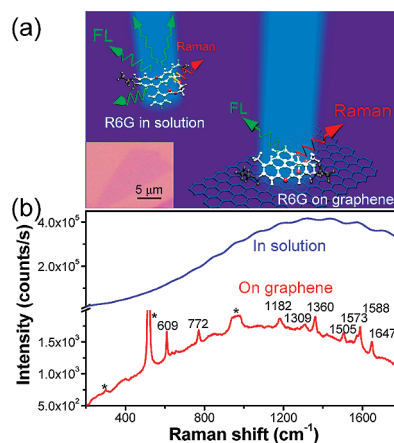


**Figure 1.** (a) Schematic illustration of graphene as a substrate to quench FL of R6G in RRS. The inset is an optical image of a 1L graphene on SiO<sub>2</sub>/Si. (b) Raman-FL spectra of R6G in water (10 μM) (blue line) and R6G on a 1L graphene (red line) at 514 nm excitation. The spectrum integration time was 10s for the blue line and 50s for the red line. The Raman peaks labeled as \* were from the SiO<sub>2</sub>/Si substrate. The 1588 cm<sup>-1</sup> peak was from graphene.

uncalibrated intensity response of our system. This uncalibrated intensity response distorts FL peaks but has a minor effect on Raman peaks because FL peaks are wide ( $>1000$  cm<sup>-1</sup>) but the Raman peaks are quite sharp ( $\sim 10$  cm<sup>-1</sup>).

In contrast, for R6G adsorbed on graphene, the FL emission was weaker and the Raman peaks were clearly observed (red line in Figure 1b). The 1588 cm<sup>-1</sup> peak was from graphene. Atomic force microscope (AFM) images of graphene before and after R6G adsorption and RRS peak assignment of R6G on graphene are in the SI.

A similar result was observed for PPP: only strong FL observed from solution (Figure 2a) vs greatly suppressed FL with moderate Raman observed from presence on graphene (Figure 2b). Assignment of RRS peaks of PPP on graphene is in the SI.

Figure 2c and 2d present Raman-FL spectra of R6G and PPP on 1L, 2L, and ML graphenes and graphite. The Raman intensity of R6G and PPP on graphite is significantly lower because of the lack of interference enhancement of excitation and signal on graphite.<sup>18</sup> Compared with ML graphene, the higher Raman intensity of R6G and PPP on 1L and 2L graphenes indicates more adsorbed R6G and PPP, which is attributed to corrugation<sup>19</sup> induced higher activity.

Compared with the solution, R6G and PPP on both graphene and graphite have a much larger Raman/FL intensity ratio. This larger Raman/FL intensity ratio may be contributed by (a) an increased RRS cross section, (b) aggregation-induced FL quenching for R6G and PPP on graphene, (c) graphene-induced FL quenching, and/or (d) photo-bleaching of R6G and PPP on graphene. First, graphene does not

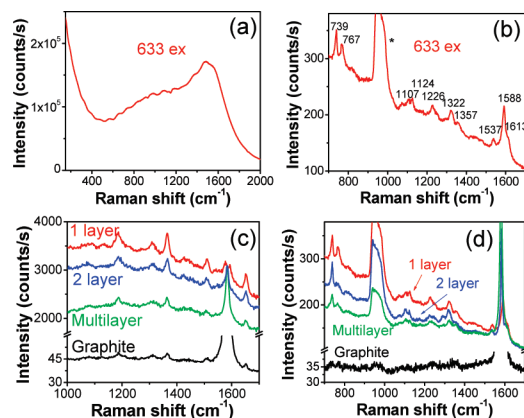


**Figure 2.** Raman-FL spectra of PPP (a) in solution and (b) on a 1L graphene at 633 nm excitation. The peak labeled as \* was from SiO<sub>2</sub>/Si. The 1588 cm<sup>-1</sup> peak was from graphene. Raman-FL spectra of (c) R6G (514 nm excitation) and (d) PPP (633 nm excitation) on different surfaces. The spectrum integration time was 2 s in (a) and 60 s in both (b) and (d). In (c), spectrum from R6G on graphite was integrated by 300 s and others were integrated by 5 s.

support electromagnetic enhancement of Raman. Chemical enhancement of Raman for graphitic material is unknown. More important, no SERS has been reported for physically adsorbed molecules on graphitic materials.<sup>20,21</sup> Therefore, the RRS cross section increase can be ruled out. Additionally, R6G does not aggregate at a concentration of 10 μM.<sup>22</sup> For PPP, a methanol solution with a low concentration was used to avoid aggregation. After adsorption, a sufficient solvent wash followed to remove nonadsorbed R6G and PPP. So aggregation is not likely here. For photobleaching of R6G and PPP on graphene, it only contributes less than 10 times to the FL suppression (see SI). Finally, the greatly increased Raman/FL intensity ratio is mainly attributed to graphene-induced FL quenching. A similar result has been reported for dyes on graphitic carbon.<sup>21</sup> For R6G on graphene, FL quenching may be mainly via energy transfer because calculation has shown a fast energy transfer from dyes to graphene<sup>23</sup> and energy transfer from R6G to metals<sup>24</sup> has usually been observed. For PPP on graphene, both energy and electron transfer are possible because both energy<sup>25</sup> and electron<sup>26</sup> transfer have been observed in a similar system (porphyrins on CNTs).

The factor of FL quenching (denoted as  $q$ ) can be calculated by

$$q = \frac{\sigma_{\text{FL in solution}}}{\sigma_{\text{FL on graphene}}} = \frac{\sigma_{\text{FL in solution}}}{\sigma_{\text{Raman on graphene}} \frac{A_{\text{FL on graphene}}}{A_{\text{Raman on graphene}}}}$$

where  $\sigma$  is the cross section and  $A$  is the integrated area. For R6G, the  $\sigma_{\text{Raman}}$  and  $\sigma_{\text{FL}}$  of R6G in solution is  $\sim 10^{-22}$  and  $\sim 10^{-16}$  cm<sup>2</sup>, respectively. The  $A_{\text{FL}}/A_{\text{Raman}}$  for R6G on graphene from 100 to 1700 cm<sup>-1</sup> (i.e., 517–564 nm) is  $\sim 10^2$ :1 (from Figure 1b). Assuming that the Raman cross section for R6G in solution and on graphene is at the same order, the FL quenching factor  $q$  can be estimated ( $q \sim 10^4$ ). Considering photobleaching contributed <10 times to FL quenching (see SI), the graphene-induced FL suppression is estimated to be  $\sim 10^3$ . Figure 3 summarizes the cross section values for R6G in solution and on graphene. A similar calculation is carried out for PPP (see SI).

In conclusion, by adsorption of R6G and PPP on graphene, we have observed RRS peaks of R6G and PPP over their FL background. The successful observation of Raman peaks is mainly attributed to graphene-induced FL quenching. Toward applications in RRS, compared with metal surfaces, graphene has its disadvantages: the lack of SERS and having interference peaks ( $\sim 1580$  and  $\sim 2700$  cm<sup>-1</sup>). However, graphene has an aromatic and hence

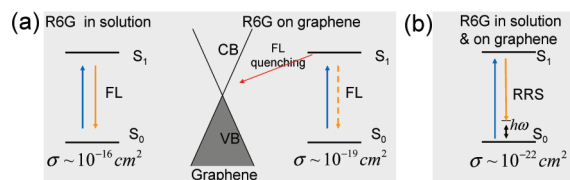


**Figure 3.** Summary of (a) FL and (b) Raman cross section of R6G in solution and on graphene. S<sub>0</sub>: ground state, S<sub>1</sub>: excited state, VB: valence band, CB: conducting band. Raman cross section of R6G in solution and on graphene is considered as the same. FL cross section of R6G on graphene is calculated using  $\sigma_{\text{FL on graphene}} = \sigma_{\text{Raman on graphene}} \frac{A_{\text{FL on graphene}}}{A_{\text{Raman on graphene}}}$ .

hydrophobic and almost nonreactive surface, which offers an alternative way for RRS measurement of fluorescent molecules.

**Acknowledgment.** This work was supported by NSFC (20673004, 20725307, and 50821061) and MOST (2006CB932701, 2006CB932403, and 2007CB936203).

**Supporting Information Available:** Chemical structures of R6G and PPP, identification of graphenes with different layers and graphite, AFM images of graphene before and after R6G adsorption, Raman peak assignment for R6G and PPP on graphene, photobleaching of R6G and PPP on graphene, estimation of the magnitude of FL suppression for PPP on graphene. This material is available free of charge via the Internet at <http://pubs.acs.org>.

## References

- (1) Benevides, J. M.; Overman, S. A.; Thomas, G. J. *J. Raman Spectrosc.* **2005**, *36* (4), 279–299.
- (2) Efremov, E. V.; Ariese, F.; Gooijer, C. *Anal. Chim. Acta* **2008**, *606* (2), 119–134.
- (3) Shim, S.; Stuart, C. M.; Mathies, R. A. *ChemPhysChem* **2008**, *9* (5), 697–699.
- (4) Parker, F. S. *Applications of Infrared, Raman and Resonance Raman Spectroscopy in Biochemistry*; Plenum Press: New York, 1983.
- (5) Matousek, P.; Towrie, M.; Ma, C.; Kwok, W. M.; Phillips, D.; Toner, W. T.; Parker, A. W. *J. Raman Spectrosc.* **2001**, *32* (12), 983–988.
- (6) Martyshkin, D. V.; Ahuja, R. C.; Kudriavtsev, A.; Mirov, S. B. *Rev. Sci. Instrum.* **2004**, *75* (3), 630–635.
- (7) McCamant, D. W.; Kukura, P.; Yoon, S.; Mathies, R. A. *Rev. Sci. Instrum.* **2004**, *75* (11), 4971–4980.
- (8) Begley, R. F.; Harvey, A. B.; Byer, R. L. *Appl. Phys. Lett.* **1974**, *25* (7), 387–390.
- (9) Nie, S. M.; Emery, S. R. *Science* **1997**, *275* (5303), 1102–1106.
- (10) Novoselov, K. S.; Geim, A. K.; Morozov, S. V.; Jiang, D.; Katsnelson, M. I.; Grigorieva, I. V.; Dubonos, S. V.; Firsov, A. A. *Nature* **2005**, *438* (7065), 197–200.
- (11) Nair, R. R.; Blake, P.; Grigorenko, A. N.; Novoselov, K. S.; Booth, T. J.; Stauber, T.; Peres, N. M. R.; Geim, A. K. *Science* **2008**, *320* (5881), 1308–1308.
- (12) Heller, D. A.; Jeng, E. S.; Yeung, T. K.; Martinez, B. M.; Moll, A. E.; Gastala, J. B.; Strano, M. S. *Science* **2006**, *311* (5760), 508–511.
- (13) Liu, Z.; Cai, W. B.; He, L. N.; Nakayama, N.; Chen, K.; Sun, X. M.; Chen, X. Y.; Dai, H. J. *Nat. Nanotechnol.* **2007**, *2* (1), 47–52.
- (14) Mohanty, N.; Berry, V. *Nano Lett.* **2008**, *8* (12), 4469–4476.
- (15) Shan, C. S.; Yang, H. F.; Song, J. F.; Han, D. X.; Ivaska, A.; Niu, L. *Anal. Chem.* **2009**, *81* (6), 2378–2382.
- (16) Gupta, A.; Chen, G.; Joshi, P.; Tadigadapa, S.; Eklund, P. C. *Nano Lett.* **2006**, *6* (12), 2667–2673.
- (17) Ni, Z. H.; Wang, H. M.; Kasim, J.; Fan, H. M.; Yu, T.; Wu, Y. H.; Feng, Y. P.; Shen, Z. X. *Nano Lett.* **2007**, *7* (9), 2758–2763.
- (18) Wang, Y. Y.; Ni, Z. H.; Shen, Z. X.; Wang, H. M.; Wu, Y. H. *Appl. Phys. Lett.* **2008**, *92* (4), 043121.
- (19) Geringer, V.; Liebmann, M.; Echtermeyer, T.; Runte, S.; Schmidt, M.; Ruckamp, R.; Lemme, M. C.; Morgenstern, M. *Phys. Rev. Lett.* **2009**, *102* (7), 076102.
- (20) Kagan, M. R.; McCreery, R. L. *Langmuir* **1995**, *11* (10), 4041–4047.
- (21) Kagan, M. R.; McCreery, R. L. *Anal. Chem.* **1994**, *66* (23), 4159–4165.
- (22) Arbeloa, F. L.; Gonzalez, I. L.; Ojeda, P. R.; Arbeloa, I. L. *J. Chem. Soc., Faraday Trans. 2* **1982**, *78*, 989–994.
- (23) Swathi, R. S.; Sebastian, K. L. *J. Chem. Phys.* **2008**, *129* (5), 054703.
- (24) Sen, T.; Patra, A. *J. Phys. Chem. C* **2008**, *112* (9), 3216–3222.
- (25) Casey, J. P.; Bachilo, S. M.; Weisman, R. B. *J. Mater. Chem.* **2008**, *18* (13), 1510–1516.
- (26) Campidelli, S.; Sooambar, C.; Diz, E. L.; Ehli, C.; Guldi, D. M.; Prato, M. *J. Am. Chem. Soc.* **2006**, *128* (38), 12544–12552.

JA9037593